Analytical Methods

Cite this: *Anal. Methods*, 2012, **4**, 3466

www.rsc.org/methods

TECHNICAL NOTE

Matrix-localization for fast analysis of arrayed microfluidic immunoassays†

Yi Zhang,‡[ae] Xuwei Wang,‡[b] Lusheng Song,[e] Chuanlai Xu,[c] Liying Ma,[d] Zhanhua Li,[b] Jianzhong Xi*[a] and Xingyu Jiang*[e]

Received 13th May 2012, Accepted 19th July 2012
DOI: 10.1039/c2ay25485a

High-throughput assays necessitate high-throughput data analysis. Arrayed microfluidic immunoassay shows the capability of high-throughput protein detection. However, its development was restricted by the low efficiency of downstream data analysis. We present herein programming-based image processing through the local recognition of a sub-array followed by the region-growing algorithm to achieve fast, convenient and precise extraction of information with reduced personal bias.

Introduction

In the early days of microarray technology, much time is spent in image analysis after obtaining the fluorescence images.[1–3] The arrayed format of images was used for high-throughput analysis of nucleic acids. For high throughput protein analysis, Bernard *et al.* reported a micromosaic immunoassay to perform the detection of model proteins by using eight-by-eight microfluidic channels.[4] This initial instance showed the potential of arrayed high-throughput immunoassays based on microfluidics. In our previous work, we developed a method that incorporates a concentration gradient generator into microfluidic networks, thus realizing the quantification of human immunodeficiency virus (HIV) antibodies from human serum.[5] To date, we are able to adapt these microfluidic devices for many assays,[6,7] but the time consumption in the final image analysis still limits the pace of our experiments. Many works improved the throughput of the microfluidic immunoassays by increasing the number of channels in the devices or the degree of automation of fluidic control,[8–11] however, many laboratories were faced with vast amounts of data that need to be dealed with by manual measurements based on packaged software of microscope.[12,13] This process is subjective and time-consuming. How to address this issue of data extraction and analysis in microfluidic immunoassays, therefore, is key to the realization of high-throughput microfluidic immunoassays.

Image segmentation refers to the recognition of region of interest (ROI) from an image, aiming for analysis and processing of the sub-images. In order to extract the information about the sub-image from the entire image, the usually used segmentation algorithms include: spectral and spatial classification, gray-scale thresholding, edge detection, region-growing, and so forth. Among them, spectral and spatial classification algorithm is normally used for color images; gray-scale thresholding algorithm binarizes the original image according to a properly determined threshold, which requires two distinct peaks in the histogram of the image; edge detection algorithm performs discrete differentiation operation on the image and recognizes the ROIs after connecting the edge points. The defect of these algorithms is the weak ability in recognizing ROIs with weak (even without) intensities. Pattern recognition and edge detection are familiar functions of many types of commercial software. However, the nonuniform background and the various shapes heavily affect the effectiveness of analysis. Some works focused on the downstream methodology for acquisition of specialized information from complicated biological images,[14–17] and showed high performance for analyzing a variety of morphologies. Compared with the lymphocyte, macrophage, vessel and neurons, arrayed spots are more orderly. Many types of high-throughout analytical data, actually, are stored as two-dimensional objects. Processing these data is a form of array manipulation, and MATLAB (abbreviation for "Matrix Laboratory"), as the name suggests, is especially adept at handling such arrayed objects.[18] Because the ROIs with the uniform size in our images are arranged as a regular array, the precise segmentation and information extraction can be achieved by fully exploiting this physical information. In this study, we utilized this feature and developed a program based on region-growing algorithm to boost the efficiency of analyzing the arrayed microfluidic immunoassays.

[a]*Department of Biomedical Engineering, College of Engineering, Peking University, Beijing 100871, China. E-mail: xi@coe.pku.edu.cn; Tel: +86-10-62760698*
[b]*State Key Laboratory for Nonlinear Mechanics, Institute of Mechanics, Chinese Academy of Sciences, Beijing 100080, China*
[c]*School of Food Science and Technology, Jiangnan University, Wuxi 214122, China*
[d]*State Key Laboratory for Infection Disease Prevention and Control, National Center for AIDS/STD Control and Prevention (NCAIDS), Chinese Center for Disease Control and Prevention (China-CDC), Beijing 102206, China*
[e]*CAS Key Lab for Biological Effects of Nanomaterials and Nanosafety, National Center for Nanoscience and Technology, Beijing 100190, China. E-mail: xingyujiang@nanoctr.cn; Fax: +86-10-82545631; Tel: +86-10-82545558*

† Electronic supplementary information (ESI) available. See DOI: 10.1039/c2ay25485a

‡ These authors contributed equally to this work.

DNA microarray images and our images from arrayed immunoassays have similarities. Because of sometimes imperfect alignment of the channels, the resulting array is not perfectly registered in lines and columns. In addition, all microarray softwares are based on the round shapes (used to analyze DNA microarrays) which will not recognize the spots in our images (which are square). We cannot employ DNA microarray software directly to analyze our image. However, from the methodological viewpoint, we are fully able to use the experience of image analysis of DNA microarray. Although there are tens of DNA microarray software, the basic steps of analysis include no more than three-steps: gridding, segmentation and intensity extraction.[1,19] The regular, unambiguous and fixed microchannel structure of arrayed microfluidics is convenient for image analysis.

Experimental

Software

Matlab is R2011b (The MathWorks Inc., USA) with Image Processing Toolbox.

Microfabrication

The microfluidic channels were fabricated *via* well-established soft lithography.[20,21] Briefly, the microchannels were designed using AutoCAD and the photomask film was printed by a commercial printer at a local company (MicroCAD Photo-Mask Ltd., China). The relief structures for the microchannels (*i.e.*, the master) were made by contact photolithography using SU-8 2100 photoresist (MicroChem) on a silicon wafer, which resulted in a height of 80 μm. We made two different microfluidic chips in this study for model titration experiment and HIV immunoassay, respectively (ESI†). The former consists of 11 channels with width of 100 μm and inter-channel distance of 200 μm (Fig. 1A); the later consists of 33 channels with width of 100 μm and inter-channel distance of 200 μm (Fig. 1B). We obtained the microfluidic channels by replica molding with polydimethylsiloxane (PDMS) prepolymer (Sylgard® 184, Dow Corning) and cured them (base : curing = 10 : 1) at 80 °C for 2 h. We punched holes for inlet and outlet of each channel and assembled channels with a flat PDMS slab. This sealing is not permanent and can be reversibly reassembled with other microfluidic channels.

Microfluidic immunoassays

We carried out the methyl paraoxon immunoassay (ESI†) using the microfluidic chip consisting of 11 channels (Fig. 1A) and the HIV immunoassay (ESI†) using the microfluidic chip consisting of 33 channels (Fig. 1B), respectively.

Programming

As described in the experimental procedure, two microfluidic chips were sealed with the same PDMS slab in the direction perpendicular to each other, successively (Scheme 1A and B). As this was a manual registration (Scheme 1B), strictly speaking, a normal image captured by microscope would be an oblique image consisting of arrayed parallelograms (Scheme 1C and Fig. 2A). Through our Matlab program (ESI†), we could easily adjust the original image and transform it into a regular array of squares (Scheme 1D and Fig. 2B). In our approach, we will first shear and rotate the image. The functions of shearing and rotation are realized by cubic spline function-based interpolation algorithm. The position of each spot is determined by region-growing algorithm. We select a sub-array consisting of $m \times n$ spots, and the position of these spots is provided by manual drawing at the ends of diagonal of the sub-array (Fig. 2C). The dimension of the spots, and the vertical and horizontal spaces between each spot within the sub-array can be determined by the

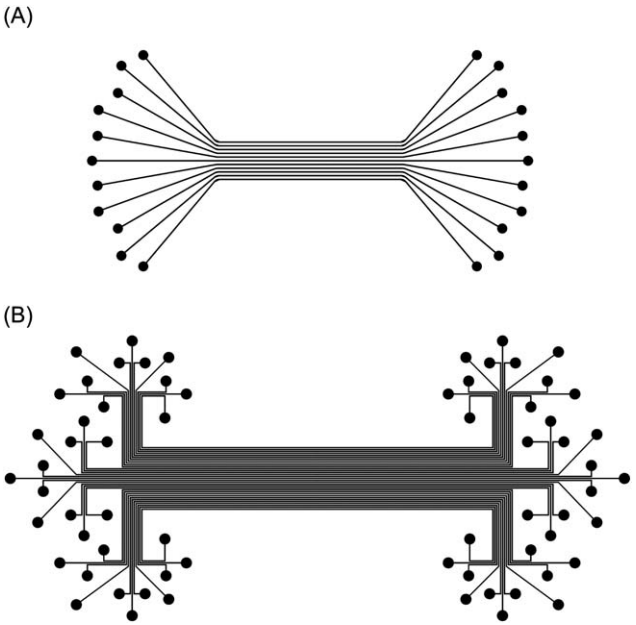

Fig. 1 The layout of the microfluidic channels. (A) 11 channels with widths of 100 μm and inter-channel distances of 200 μm. (B) 33 channels with widths of 100 μm and inter-channel distances of 200 μm.

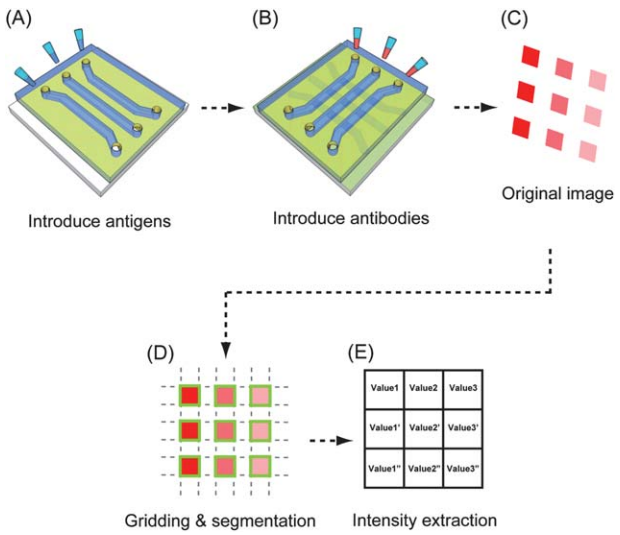

Scheme 1 The schematic diagram of arrayed immunoassay (A–C) followed by image processing (D and E).

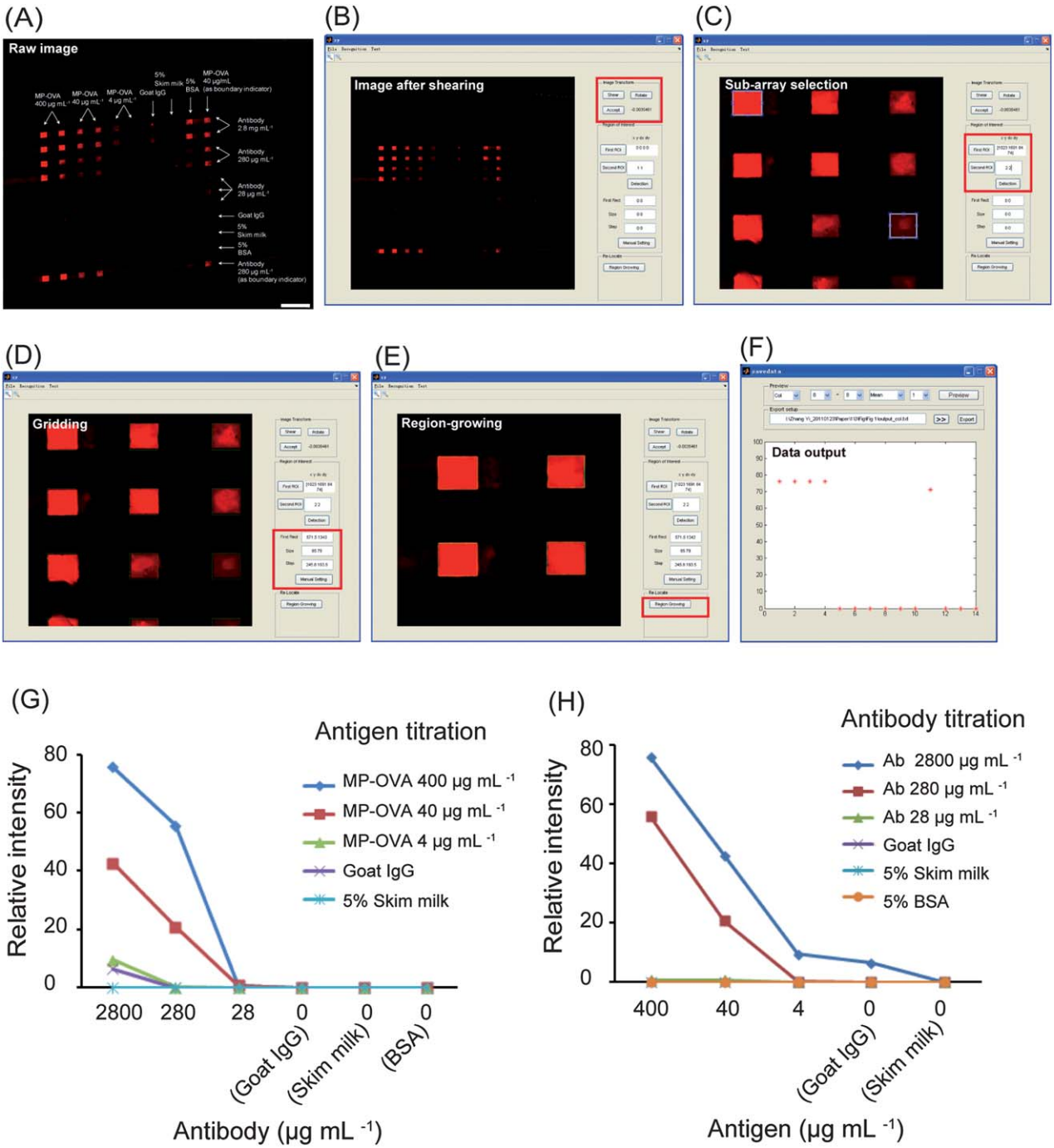

Fig. 2 The methyl paraoxon antigen–antibody titration. (A) The original image of antigen–antibody titration experiment consists of 10 × 11 array. The scale bar is 500 μm. (B) Shearing result of the image. (C) Manual selection of the ends of diagonal of the sub-array. (D) Manual adjustments for gridding. (E) Region-growing for the spots. (F) Data output based on either reference row or reference column. (G) Antigen titration curve. (H) Antibody titration curve.

program. The center of the spot will be given as the "seed" of region-growing. According to the determined parameters above, the final gridding for each spot of the image is given by growing the seeds on the binarized image which is given by the 1/4 maximum gray value (Fig. 2D and E). After the region-growing, the program will compare the length/width of each spot with the others at the same column/row. If it is far away (*i.e.*, with 60% deviation) from average value of the length/width of spots at the same column/row, the recognized size will be abandoned. At last, the program could output the gray value as a matrix (Scheme 1E and Fig. 2F) which accords with the adjusted image. In addition, the program could specify a row/column as negative or blank control, and the output data will be subtracted the corresponding mean or median value of pixels within the spot.

Results and discussion

Antigen–antibody titration

In immunoassays, researchers typically have to explore the optimal concentration of specific antigen or antibody. This work is labor-intensive and often requires a lot of time by using 96-well plates. In order to decrease the time consumption and to eliminate errors between different batches of experiments, we utilized the microfluidic system to improve the traditional approach.

Methyl paraoxon (MP) is an organophosphorus pesticide and is toxic to humans. An indirect enzyme-linked immunosorbent assay (indirect ELISA) for methyl paraoxon has been developed recently.[22] The investigation for optimal concentration of antigen–antibody in microfluidic chips can be highly efficient compared to carrying out this optimization in 96-well plate. Fig. 2A showed the original image of the titration experiment. Each gradient solution was introduced in parallel and we took the average value of four spots as the final value for each concentration. From the image, we also found that BSA is unsuited as a blocking reagent since the MP antibody could bind to BSA (Fig. 2A). We set 5% skim milk as the negative control because it has no cross-reactivity with the MP antibody. Fig. 2B–F showed the sequential analysis of the image at the Matlab GUI (graphical user interface), including (1) the shearing (Fig. 2B), (2) the selection of sub-array (Fig. 2C), (3) the adjustment of the position of origin, the length/width of the spot, and the space between adjacent spots (Fig. 2D), (4) the region-growing (Fig. 2E), and (5) the data output (Fig. 2F). When we optimize the concentration of antigen, we set vertical column "5% skim milk" as the negative control, and set 1st antibody dilutions as the horizontal axis. The resulting curve of antigen (Fig. 2G) showed that 40 μg mL^{-1} is the optimal concentration of MP-OVA (methyl paraoxon conjugated with ovalbumin) since it has the best linearity compared with others. When we optimize the concentration of antibody, we should make horizontal row "5% skim milk" as the negative control, and set antigen dilutions as the horizontal axis. The resulting curve of antibody titration (Fig. 2H) indicated that 280 μg mL^{-1} is the optimal concentration of 1st antibody because of its good linearity and low background. So we are able to obtain the optimal concentration of antigen and antibody through one experiment. The program improves the efficiency of analysis markedly.

High-throughput HIV detection

Microfluidic channels allow rapid analysis of pairs of antigen–antibody interactions. We focused on major diseases related to human health such as AIDS caused by HIV.[23] Microfluidic devices provide a powerful tool for high-throughput biomedical diagnosis. In this study, we tested 30 human sera simultaneously, and analyzed the result using the developed program. Fig. 3A shows the comprehensive test of HIV antibodies in human sera against seven HIV surface antigens: p24, p31, gp41, p51, p55, gp120, and gp36. p24, p31, gp41, p51, p55, and gp120 are HIV-1 specific biomarkers; gp36 is a HIV-2 specific biomarker. We analyzed the image under the GUI environment by the similar operation above, and the output data and the corresponding column diagram are shown in Table S1† and Fig. 3B, respectively. We set the HIV- serum as the negative control when we output the gray values of each spot. From Fig. 3B, we could

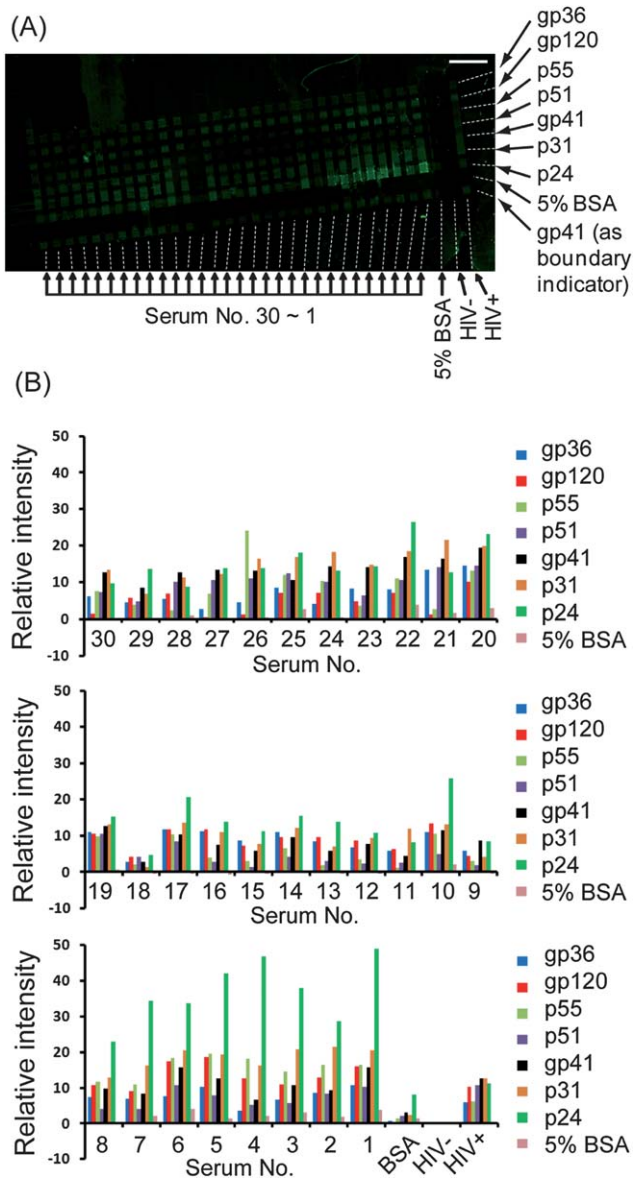

Fig. 3 The HIV-1/2 antibodies immunoassay of 30 sera. (A) The original image consists of 33 × 9 arrays captured by microscope. The scale bar is 500 μm. (B) The statistical chart of result. 7 targets for 33 samples (including negative/positive controls) were plotted, based on the output text file shown in Table S1†.

estimate that 29 specimens (serum no. 1–17, 19–30) are HIV-1/2 positive, 1 specimen (serum no. 18) is HIV-1 uncertain and HIV-2 negative, according to the Section 5.1.2.5 of the National Guideline for Detection of HIV/AIDS released by Chinese Center for Disease Control and Prevention (China CDC).[24] The guideline prescribes that the HIV-1 infection can be confirmed when (1) both anti-gp41 antibody and anti-gp120 antibody exist, (2) both anti-p24 antibody and either anti-gp41 antibody or anti-gp120 antibody exist.

Conclusions

Microfluidic devices have expanded the throughput for immunoassays. In this work, we focused on the downstream data

extraction and developed a Matlab-based program. This program possesses the function of adjusting, gridding, and correcting images consisting of arrayed spots. The crucial part of the program is the localization (*i.e.*, the determination of coordinates) of each reaction spot. We determined the dimension and the position of the seed for a sub-array, which reduced the time consumption for image processing and overcame the difficulties resulted from the partial region with low signal-to-noise ratio. The extraction of gray value can be easily done after the matrix localization. Using this program, we realized the high-throughput antigen–antibody titration and the HIV antibody detection, from upstream to downstream of the whole procedure. No matter how high the throughput is, the total time of immunoassay is about 1 hour. The time consumption in image analysis is only about 3–5 minutes which depends on the number of pixels in the captured image. Our study gives an approach that will contribute to the improvement of the entire efficiency of the high-throughput immunoassay.

Acknowledgements

We thank Dr. Kang Sun for the helpful suggestions about microfabrication. We thank Mr. Sha He and Dr. Jiashu Sun for proofreading. We thank the Ministry of Science and Technology (2009CB930001, 2011CB933201), National Science Foundation of China (51073045, 21025520, 20890020, 90813032, 21105018), the Chinese Academy of Sciences (KJCX2-YW-M15) and the Novo Nordisk-CAS Research Foundation (NNCAS-2010-5) for financial help.

Notes and references

1 Y. H. Yang and T. Speed, in *DNA Microarrays: A Molecular Cloning Manual*, ed. D. Bowtell and J. Sambrook, Cold spring Harbor Laboratory Press, New York, 2003, pp. 526–535.
2 M. J. Heller, *Annu. Rev. Biomed. Eng.*, 2002, **4**, 129–153.
3 M. Schena, D. Shalon, R. W. Davis and P. O. Brown, *Science*, 1995, **270**, 467–470.
4 A. Bernard, B. Michel and E. Delamarche, *Anal. Chem.*, 2000, **73**, 8–12.
5 X. Y. Jiang, J. M. K. Ng, A. D. Stroock, S. K. W. Dertinger and G. M. Whitesides, *J. Am. Chem. Soc.*, 2003, **125**, 5294–5295.
6 Y. Sun, Y. Y. Liu, W. S. Qu and X. Y. Jiang, *Anal. Chim. Acta*, 2009, **650**, 98–105.
7 Y. Y. Liu, Y. Sun, K. Sun, L. S. Song and X. Y. Jiang, *J. Mater. Chem.*, 2010, **20**, 7305–7311.
8 E. P. Kartalov, J. F. Zhong, A. Scherer, S. R. Quake, C. R. Taylor and W. F. Anderson, *BioTechniques*, 2006, **40**, 85–90.
9 J. Kong, L. Jiang, X. O. Su, J. H. Qin, Y. G. Du and B. C. Lin, *Lab Chip*, 2009, **9**, 1541–1547.
10 M. Ikami, A. Kawakami, M. Kakuta, Y. Okamoto, N. Kaji, M. Tokeshi and Y. Baba, *Lab Chip*, 2010, **10**, 3335–3340.
11 J. Yan, M. Hu, D. Li, Y. He, R. Zhao, X. Y. Jiang, S. P. Song, L. H. Wang and C. H. Fan, *Nano Res.*, 2008, **1**, 490–496.
12 Y. Y. Liu, J. Yu, M. H. Du, W. J. Wang, W. Zhang, Z. Wang and X. Y. Jiang, *Biomed. Microdevices*, 2012, **14**, 17–23.
13 Y. Y. Liu, D. Y. Yang, T. Yu and X. Y. Jiang, *Electrophoresis*, 2009, **30**, 3269–3275.
14 K. M. Kim, S. Y. Kim, J. Minxha and G. T. R. Palmore, *J. Neurosci. Methods*, 2011, **201**, 98–105.
15 M. A. Alyassin, S. Moon, H. O. Keles, F. Manzur, R. L. Lin, E. Haeggstrom, D. R. Kuritzkes and U. Demirci, *Lab Chip*, 2009, **9**, 3364–3369.
16 J. Selinummi, P. Ruusuvuori, I. Podolsky, A. Ozinsky, E. Gold, O. Yli-Harja, A. Aderem and I. Shmulevich, *PLoS One*, 2009, **4**, e7497.
17 M. E. Seaman, S. M. Peirce and K. Kelly, *PLoS One*, 2011, **6**, e20807.
18 E. A. Sobie, *Sci. Signaling*, 2011, **4**, tr7.
19 D. V. Nguyen, A. B. Arpat, N. Wang and R. J. Carroll, *Biometrics*, 2002, **58**, 701–717.
20 Y. N. Xia and G. M. Whitesides, *Annu. Rev. Mater. Sci.*, 1998, **28**, 153–184.
21 K. Sun, Z. X. Wang and X. Y. Jiang, *Lab Chip*, 2008, **8**, 1536–1543.
22 Z. K. Li, Y. Y. Zhu, X. G. Yin, C. F. Peng, W. Chen, L. Q. Liu, L. M. Yin and C. L. Xu, *Immunol. Invest.*, 2009, **38**, 510–525.
23 D. Y. Yang, X. Niu, Y. Y. Liu, Y. Wang, X. Gu, L. S. Song, R. Zhao, L. Y. Ma, Y. M. Shao and X. Y. Jiang, *Adv. Mater.*, 2008, **20**, 4770–4775.
24 National Guideline for Detection of HIV/AIDS (2009 version), http://www.chinaids.org.cn/n16/n1193/n4073/n299951.files/n299950.doc.

